

SOURCE-OPTIMAL TRAINING IS TRANSFER-SUBOPTIMAL

C. Evans Hedges

ABSTRACT. We prove a fundamental misalignment in transfer learning: the source regularization that minimizes source risk almost never coincides with the regularization maximizing transfer benefit. Through sharp phase boundaries for L2-SP ridge regression, we characterize the transfer-optimal source penalty τ_0^* for a fixed task alignment. With sufficiently weak alignment, τ_0^* is always larger than the source optimal regularization, however with strong alignment τ_0^* diverges predictably from task-optimal values: requiring stronger regularization in high-SNR regimes and weaker regularization in low-SNR regimes. Additionally, in isotropic settings the decision to transfer is remarkably independent of target sample size and noise, depending only on task alignment and source characteristics. CIFAR-10 and MNIST experiments confirm this counterintuitive pattern persists in non-linear networks.

Keywords: Transfer learning, ridge regression, overparameterization, L2-SP, phase boundaries, random matrix theory, pretraining, continual learning, deterministic equivalents.

1. INTRODUCTION

1.1. Background and Motivation. A fundamental question in transfer learning is: how should we train the source model to maximize downstream performance? Conventional wisdom suggests optimizing the source task leads to better transfer. We prove the opposite: the source regularization that minimizes source risk almost never coincides with the regularization that maximizes transfer benefit. This misalignment occurs in a predictable way depending on the source noise and task alignment. In the setting of high task alignment, optimal source training for transfer counterintuitively requires more regularization when the source has high SNR and less regularization in the high-noise regime.

We begin our exploration through the lens of evaluating when we would expect positive or negative transfer from some source task to a target task. Previous work [5, 13, 16] has shown that the phenomenon of negative transfer is a concern, where the model generated by transfer learning performs worse than if one were to train the model from scratch. Intuition and previous theoretical work [13] suggest that if the tasks and input datasets are similar enough, transfer learning techniques should help, but if the target task is sufficiently different, or in the context of continual learning the regime has shifted enough, transfer learning may harm the final model, introducing bias and noise from the initialization.

There has been notable work examining this phase boundary between when one should expect positive or negative transfer. In [5, 6], Dar and Baraniuk provided an explicit quantitative phase boundary for freezing/parameter-sharing style transfer in linear models, giving if-and-only-if conditions for when shared representations outperform training from scratch. In [7], Dhifallah and Lu explored the phenomenon in the context of feature freezing. Additionally, feature-overlap driven transitions in linear transfer were explored by Tahir, Ganguli, and Rotskoff in [14]. Related phase transitions have been characterized for other linear transfer mechanisms such as hard parameter sharing [16]. Complementary asymptotic analyses

Date: November 25, 2025.

for fine-tuning from pretrained anchors via gradient descent appear in Ghane, Akhtiamov, and Hassibi [9], who provide universal asymptotics comparing pretrained versus fine-tuned models under distributional shifts.

The L2-SP (L2-distance to Starting Point) approach was introduced by Li, Grandvalet, and Davoine [15], who showed empirical improvements by penalizing deviation from pretrained parameters. This approach matches many practical fine-tuning protocols and corresponds to the isotropic elastic weight consolidation (EWC) penalty [11]. Dar, LeJeune, and Baraniuk [6] recently analyzed when L2-SP transfer learning outperforms standard ridge regression, assuming task parameters are related by orthonormal transformations and focusing on optimal tuning of the target-task regularization given a fixed source model.

Our work extends this analysis in several critical directions. First, we consider arbitrary task vectors without orthonormal structure, covering realistic scenarios where tasks differ in both magnitude and direction. Second, we provide sharp if-and-only-if boundaries characterizing exactly when transfer outperforms training from scratch, in both finite-sample and deterministic-equivalent settings. Third, and most significantly, we address the source-side optimization problem: how should one train the source model to maximize downstream transfer benefit? Given the alignment of two tasks, we derive the transfer-optimal source regularization τ_0^* and prove it generically differs from the source-task-optimal choice, revealing a fundamental misalignment between optimizing for source performance versus transfer capability. This source-side perspective appears to be entirely novel, as prior work focuses on target-task tuning given a pre-trained source model.

1.2. Setup and Overview of Results. In this paper we formalize transfer learning from the lens of L2-SP ridge regression. In particular, we have two tasks, Task 0 (the source task) and Task 1 (the target task), as well as corresponding training datasets (X_0, y_0) and (X_1, y_1) . We then seek to evaluate the expected out-of-sample risk on Task 1, comparing the ridge/ridgeless solution trained solely on (X_1, y_1) to the L2-SP ridge solution found by first training a ridge/ridgeless model on (X_0, y_0) , and then using those model parameters as the prior for ridge/ridgeless training on (X_1, y_1) .

Our analysis builds on the foundational work characterizing ridge and ridgeless regression risk in high-dimensional settings [8, 10], which established the precise asymptotic behavior of these estimators in overparameterized regimes and revealed phenomena such as double descent [3] and benign overfitting [2]. We employ random matrix theory techniques, specifically the deterministic equivalent framework [1, 4, 8, 10], to derive precise asymptotic characterizations of the estimators' risk and identify sharp phase boundaries for transfer benefit.

Our contributions can be outlined as follows. First, Theorem 3.3 provides an if-and-only-if inequality describing when transfer learning will outperform from-scratch training in the finite data, non-isotropic ridge regime. As a corollary, we show that in the finite sample, isotropic, ridgeless case the inequality takes a simple form and is interestingly independent of n_1 and σ_1 . This independence is consistent with prior isotropic analyses of freezing-style transfer [5, 13], and our finite-sample isotropic/ridgeless corollary recovers these patterns in the L2-SP setting.

We then examine deterministic equivalents in the asymptotic limit and Theorem 3.6 provides a DE characterization and asymptotic boundary for L2-SP ridge transfer with general (non-orthonormal) task vectors. Corollary 3.7 examines the isotropic case, where the decision criterion is determined entirely by whether or not the alignment of the two tasks surpasses a bias and noise term dependent only on Task 0.

From this we arrive at Theorem 3.8, which identifies the unique τ_0^* (source model ridge penalty) that maximizes transfer benefit, given a particular task alignment. Outside of a measure-zero set, τ_0^* does not coincide with the optimal Task 0 ridge parameter, and notably τ_0^* is independent of target sample size but depends on task alignment. Together, these results give the first explicit analytical boundary for when Euclidean L2-SP transfer helps with general (non-orthonormal) task vectors in overparameterized ridge models, including general covariance and DE limits, and provide surprising insights into optimally training source models for the purpose of transfer learning.

Finally, we establish in Corollary 3.9 that under sufficiently aligned tasks, in the high-SNR regime (low noise) τ_0^* is greater than the source-optimal ridge penalty, and similarly in the low-SNR regime (high noise), τ_0^* is less than the source-optimal ridge penalty. Additionally, with poor alignment τ_0^* is always larger than the source-optimal ridge penalty.

Though derived in linear models, these results isolate a core mechanism that likely persists in overparameterized nonlinear networks. Additionally although standard SGD fine-tuning protocols do not necessarily use an L2-SP penalty, this mechanism models the implicit regularization of SGD fine-tuning where the optimization trajectory remains anchored in the basin of the initialization. We validate the conjecture that the SNR- τ_0^* relationship observed in Corollary 3.9 holds in non-linear networks through experiments on CIFAR-10 and MNIST (Section 4), which provides further evidence of the SNR-dependent pattern. This suggests that our theoretical work may provide analytical foundations for understanding regularization design in pre-training pipelines.

The remainder of the paper is outlined as follows. Section 2 sets up the model and assumptions. Section 3 presents the core mathematical results. Section 4 provides empirical validation of our theoretical predictions on CIFAR-10 and MNIST. We conclude with Section 5 and discuss implications and limitations; proofs are deferred to the Appendix.

2. PRELIMINARIES

We let Z_0, Z_1 be $n_0, n_1 \times p$ random matrices with entries taken iid with mean 0, variance 1, and finite $2 + \epsilon$ moments and Lindeberg condition (see [1] for more information). These assumptions are sufficient for the deterministic equivalents we will examine later, but it is safe also to simplify these assumptions taking entries in Z_i to be iid $N(0, 1)$. We additionally assume we are in the overparameterized regime, with $n_0, n_1 < p - 1$. We let Σ_0, Σ_1 be covariance matrices and $X_i = Z_i \Sigma_i^{1/2}$. Next we have true signal vectors w_0, w_1 and let $y_i = X_i w_i + \epsilon_i$ where $\epsilon_i \sim N(0, \sigma_i^2 I)$.

We adopt the L2-SP approach found in [15] and examine the following estimators:

$$\hat{\beta}_0(\lambda_0) := \arg \min_{\beta} \|y_0 - X_0 \beta\|^2 + \lambda_0 \|\beta\|^2 = (X_0^\top X_0 + \lambda_0 I)^{-1} X_0^\top y_0,$$

$$\hat{\beta}_1^S(\lambda_1) := \arg \min_{\beta} \|y_1 - X_1 \beta\|^2 + \lambda_1 \|\beta\|^2 = (X_1^\top X_1 + \lambda_1 I)^{-1} X_1^\top y_1,$$

$$\begin{aligned} \hat{\beta}_1^{TL}(\lambda_1 \mid \hat{\beta}_0) &:= \arg \min_{\beta} \|y_1 - X_1 \beta\|^2 + \lambda_1 \|\beta - \hat{\beta}_0(\lambda_0)\|^2 \\ &= (X_1^\top X_1 + \lambda_1 I)^{-1} (X_1^\top y_1 + \lambda_1 \hat{\beta}_0(\lambda_0)). \end{aligned}$$

We also will take the notation that $\hat{\beta}_0(0) = \lim_{\lambda_0 \searrow 0} \hat{\beta}_0(\lambda_0)$ represents the ridgeless estimator (and similarly for $\hat{\beta}_1^S$ and $\hat{\beta}_1^{TL}$). In this setting of course $\hat{\beta}_0$ represents our ridge/ridgeless

estimator for Task 0, $\hat{\beta}_1^S$ is our standard ridge/ridgeless estimator for Task 1, and $\hat{\beta}_1^{TL}$ is our transfer learning estimator for Task 1 that takes the solution of Task 0 as its prior.

We note here that $\hat{\beta}_1^{TL}(\lambda_1 | \hat{\beta}_0)$ corresponds exactly to the MAP estimator with Gaussian prior $\beta \sim N(\hat{\beta}_0, \lambda_1^{-1}I)$ and matches practical L2-SP fine-tuning [15] and the isotropic EWC penalty [11]. We also note that we do not reweight our penalty by a task metric H and stick with standard Euclidean distancing for our ridge penalty. This differs from the whitened/metric-based formulations and also more accurately reflects typical implementations of L2-SP and fine-tuning where the penalty is applied in Euclidean parameter space without whitening.

To evaluate out-of-sample performance of these estimators we will use their expected prediction risk:

$$\text{Risk}_1(\beta) := \mathbb{E}_{x_1 \sim N(0, \Sigma_1)}[(x_1^\top \beta - x_1^\top w_1)^2] = \|\beta - w_1\|_{\Sigma_1}^2,$$

where $\|v\|_\Sigma^2 = v^\top \Sigma v$.

Our first goal is to understand when L2-SP transfer improves expected Task 1 risk, namely when

$$\text{Risk}_1(\hat{\beta}_1^S(\lambda_1)) > \text{Risk}_1(\hat{\beta}_1^{TL}(\lambda_1 | \hat{\beta}_0(\lambda_0))).$$

We will additionally make use of the Frobenius norm in Σ geometry, which we will denote as follows:

$$\|A\|_{\Sigma, F}^2 = \text{Tr}(A^\top \Sigma A).$$

Finally, some common matrices we will be using deserve their own notation, and we define that here: let

$$M_{\lambda_1}^{(i)} = (X_i^\top X_i + \lambda_1 I)^{-1}$$

and note that

$$M_{\lambda_1}^{(1)} X_1^\top X_1 - I = -\lambda_1 M_{\lambda_1}^{(1)}.$$

Additionally let

$$P_i = X_i^+ X_i,$$

where X_i^+ is the Moore-Penrose pseudoinverse, so that P_i is the orthogonal projector in \mathbb{R}^p onto $\text{row}(X_i)$ and $I - P_i$ projects onto $\ker(X_i)$.

3. MATHEMATICAL RESULTS

3.1. Finite Sample Risk Formulas. First we recall the expected out of sample risk of ridge regression (see [10] for a modern reference)

Observation 3.1. *The expected risk of ridge regression is*

$$R^S(\lambda_1) = \lambda_1^2 \mathbb{E} \left[\|M_{\lambda_1}^{(1)} w_1\|_{\Sigma_1}^2 \right] + \sigma_1^2 \mathbb{E} \left[\|M_{\lambda_1}^{(1)} X_1^\top\|_{\Sigma_1, F}^2 \right].$$

Next we compute the finite sample risk for L2-SP ridge regression:

Lemma 3.2. *The expected risk of the transfer estimator decomposes into pure bias, variance induced by the β_0 prior, and variance induced by estimation error:*

$$R^{TL}(\lambda_1) = B^{TL}(\lambda_1) + \sigma_0^2 V_0^{TL}(\lambda_1) + \sigma_1^2 V_1^{TL}(\lambda_1)$$

with:

$$\begin{aligned} B^{TL}(\lambda_1) &= \lambda_1^2 \mathbb{E} \left[\|M_{\lambda_1}^{(1)} M_{\lambda_0}^{(0)} X_0^\top X_0 w_0 - M_{\lambda_1}^{(1)} w_1\|_{\Sigma_1}^2 \right] \\ V_0^{TL}(\lambda_1) &= \lambda_1^2 \mathbb{E} \left[\|M_{\lambda_1}^{(1)} M_{\lambda_0}^{(0)} X_0^\top\|_{\Sigma_1, F}^2 \right] \\ V_1^{TL}(\lambda_1) &= \mathbb{E} \left[\|M_{\lambda_1}^{(1)} X_1^\top\|_{\Sigma_1, F}^2 \right]. \end{aligned}$$

The following theorem characterizes when transfer helps by comparing the bias introduced by starting from zero (standard ridge) versus starting from the source parameters (L2-SP). Transfer succeeds when the alignment between the tasks, after appropriate filtering through the ridge resolvent and covariance geometry, exceeds a threshold determined by source bias and noise. Note that since the Task 1 variance portion of risk for both of these estimators is the same, it is independent from the decision of whether or not transfer will benefit.

Theorem 3.3. *In the finite sample case with $\lambda_1 > 0$, we gain benefit from transfer learning ($R^{TL}(\lambda_1) < R^S(\lambda_1)$) if and only if:*

$$2\mathbb{E} \left[\langle M_{\lambda_1}^{(1)} M_{\lambda_0}^{(0)} X_0^\top X_0 w_0, M_{\lambda_1}^{(1)} w_1 \rangle_{\Sigma_1} \right] > \mathbb{E} \left[\|M_{\lambda_1}^{(1)} M_{\lambda_0}^{(0)} X_0^\top X_0 w_0\|_{\Sigma_1}^2 \right] + \sigma_0^2 \mathbb{E} \left[\|M_{\lambda_1}^{(1)} M_{\lambda_0}^{(0)} X_0^\top\|_{\Sigma_1, F}^2 \right].$$

As a corollary, in the ridgeless limit we consider when X_i is taken to be isotropic and Gaussian so that the Wishart formulas apply exactly:

Corollary 3.4. *In the finite case, if $\Sigma_i = I$ and $\lambda_1 = \lambda_0 = 0$ and X_i is taken to be Gaussian, then $R^{TL}(0) < R^S(0)$ if and only if:*

$$2 \langle w_0, w_1 \rangle > \|w_0\|^2 + \sigma_0^2 \frac{p}{p - n_0 - 1}.$$

A noteable feature of the isotropic ridgeless boundary is its complete independence from n_1 and σ_1 : the transfer decision depends only on task alignment $\langle w_0, w_1 \rangle$ and source characteristics ($\|w_0\|, \sigma_0, n_0, p$). This independence has surprising practical implications: if transfer outperforms training from scratch with 10 target samples, it remains beneficial with 1,000 samples. Conversely, if tasks are misaligned enough that transfer fails with limited data, collecting more target data will not remedy the situation, only improving task alignment or source model quality will help. We also observe here that the transfer region monotonically shrinks as σ_0 grows. Thus, in order to maximize the potential transfer benefit it is essential to ensure source task noise is as small as possible.

3.2. Deterministic Equivalents and Asymptotics. We will now examine asymptotics for the ridge phase transition identified above and use deterministic equivalents to understand the limiting phase transition. To establish the core deterministic equivalents, we will scale our λ_i with n_i and let $\tau_i = \lambda_i/n_i$. We define the following ridge resolvent:

$$Q_i(\tau_i) = (\tau_i I + \delta_i(\tau_i) \Sigma_i)^{-1}$$

where $\delta_i(\tau_i)$ is the unique positive solution to the Silverstein fixed-point equation

$$\delta_i(\tau_i) = n_i \text{Tr} \left(\Sigma_i (\tau_i I + \gamma_i \delta_i(\tau_i) \Sigma_i)^{-1} \right), \text{ where } \gamma_i = \lim p/n_i.$$

We will use the notation $A_n \asymp B_n$ to denote deterministic equivalent convergence, meaning that for any sequence of deterministic matrices D_n with uniformly bounded spectral norm, we have $\text{Tr}(D_n(A_n - B_n)) \rightarrow 0$ almost surely as $n \rightarrow \infty$. This is the standard notion of weak deterministic equivalence used in random matrix theory [1].

First, the following deterministic equivalents will be useful:

Observation 3.5. *Under standard Bai-Silverstein conditions ([1]), as $p, n_i \rightarrow \infty$ with $p/n_i \rightarrow \gamma_i$:*

$$\begin{aligned} \lambda_1 M_{\lambda_1}^{(1)} &\asymp \tau_1 Q_1(\tau_1), \\ M_{\lambda_0}^{(0)} X_0^\top &\asymp n_0^{-1} \frac{1}{\tau_0(1 + \delta_0(\tau_0))} X_0^\top, \text{ and} \\ M_{\lambda_0}^{(0)} X_0^\top X_0 M_{\lambda_0}^{(0)} &\asymp n_0^{-1} (Q_0(\tau_0) - \tau_0 Q_0(\tau_0)^2). \end{aligned}$$

Finally, define

$$t(\tau_0, \tau_1) = \lim_{p \rightarrow \infty} p^{-1} \text{Tr} (Q_1(\tau_1) \Sigma_1 Q_1(\tau_1) (Q_0(\tau_0) - \tau_0 Q_0(\tau_0)^2)).$$

Under the Bai-Silverstein assumptions, the eigenvalue distributions of Σ_0 and Σ_1 converge weakly and the resolvents $Q_i(\tau_i)$ are uniformly bounded, ensuring that this limit exists and equals the limit of the corresponding trace per dimension. By independence of X_0 and X_1 , we may substitute these deterministic equivalents into the results from Theorem 3.3 to arrive at the following asymptotic decision criterion:

Theorem 3.6. *In the asymptotic limit, we gain benefit from transfer learning ($R^{TL}(\lambda_1) < R^S(\lambda_1)$) if and only if:*

$$2 \langle Q_1(\tau_1)(I - \tau_0 Q_0(\tau_0))w_0, Q_1(\tau_1)w_1 \rangle_{\Sigma_1} > \|Q_1(\tau_1)(I - \tau_0 Q_0(\tau_0))w_0\|_{\Sigma_1}^2 + \sigma_0^2 \gamma_0 t(\tau_0, \tau_1).$$

And in the isotropic case:

Corollary 3.7. *In the isotropic case where $\Sigma_0 = \Sigma_1 = I$, we (asymptotically) gain benefit from transfer learning ($R^{TL}(\lambda_1) < R^S(\lambda_1)$) if and only if:*

$$2 \langle w_0, w_1 \rangle > \gamma_0 a_0^2 \|w_0\|^2 + \sigma_0^2 \gamma_0 a_0,$$

where

$$a_0 = \frac{-\tau_0 + \sqrt{\tau_0^2 + 4\gamma_0}}{2\gamma_0}.$$

As in the finite sample isotropic ridgeless case, in the isotropic DE (ridge) setting this decision boundary is independent of τ_1 , γ_1 , and σ_1 . This remarkable independence implies that if there exists any ridge penalty τ_1 for which transfer outperforms from-scratch training, then transfer is universally beneficial regardless of target-task regularization.

As in the finite sample isotropic ridgeless case, alignment of the two tasks must pass a threshold that is independent of the target task. This transfer benefit region is again monotonically shrinking in σ_0 , and may be maximized by minimizing the quantity on the right. By fixing γ_0 we arrive at the following result:

Theorem 3.8. *In the asymptotic setting with isotropic data and fixed source model over-parameterization γ_0 , for any fixed target task alignment $\rho = \langle w_0, w_1 \rangle$, there exists a unique source ridge penalty τ_0^* that maximizes the transfer benefit $\Delta R = R^S - R^{TL}$. Additionally, outside of a measure-zero set of parameters, the optimal τ_0^* for transfer learning differs from the optimal ridge penalty for Task 0 performance.*

As a corollary, we identify that there are two notable alignment regimes. In the poorly aligned case, transfer optimal regularization is always stronger than source optimal regularization.

In the well aligned case the situation requires more nuance, with transfer requiring more regularization than source optimal in the low noise regime and requiring less regularization than expected in the high noise regime.

Corollary 3.9. *Assume $\|w_0\|^2 > \langle w_0, w_1 \rangle > 0$.*

If $\langle w_0, w_1 \rangle < \frac{3}{4} \|w_0\|^2$, then $\tau_0^ > \frac{\gamma_0 \sigma_0^2}{\|w_0\|^2}$ (transfer optimal always requires stronger regularization when the tasks have poor alignment).*

However, with sufficient alignment ($\langle w_0, w_1 \rangle > \frac{3}{4} \|w_0\|^2$) there exists an noise threshold $\sigma_0^ > 0$ identified by*

$$(\sigma_0^*)^2 = \frac{2 (\|w_0\|^4 - \|w_0\|^2 \langle w_0, w_1 \rangle)}{\sqrt{\gamma_0 (\|w_0\|^2 \langle w_0, w_1 \rangle - \frac{3}{4} \|w_0\|^4)}}$$

such that:

- If $\sigma_0 < \sigma_0^*$, then $\tau_0^* > \frac{\gamma_0 \sigma_0^2}{\|w_0\|^2}$ (stronger regularization than source-optimal).
- If $\sigma_0 > \sigma_0^*$, then $\tau_0^* < \frac{\gamma_0 \sigma_0^2}{\|w_0\|^2}$ (weaker regularization than source-optimal).

In particular, this shows that when the tasks are appropriately aligned ($\langle w_0, w_1 \rangle > \frac{3}{4} \|w_0\|^2$), if the source task has low SNR, τ_0^* is actually less than the task-optimal ridge penalty, indicating that in the noisy regime the transfer-optimal solution actually uses less regularization than one would typically use for source task alone, and similarly for the high SNR regime.

4. EMPIRICAL VALIDATION

While our theoretical analysis focuses on linear ridge regression, a natural question is whether the core phenomenon, that source-optimal regularization differs from transfer-optimal regularization, persists in more realistic nonlinear settings. We provide empirical evidence on two datasets, CIFAR-10 and MNIST, to test whether the SNR-dependent pattern predicted by Corollary 3.9 extends beyond the linear regime. Figure 1 summarizes our empirical findings across both datasets. We employ these controlled, small-scale setups specifically to isolate the regularization mechanism from confounding factors like feature learning dynamics or massive pre-training scale. We note that while standard fine-tuning uses SGD without an explicit L2-SP penalty, for limited training horizons the optimization implicitly regularizes towards the initialization, functionally approximating the L2-SP constraint analyzed in our theory.

4.1. CIFAR-10 Experiments.

4.1.1. *Experimental Setup.* We construct a transfer learning task with high alignment using CIFAR-10 [12] by splitting the 10 classes into two groups: a source task consisting of animal classes (bird, cat, deer, dog, frog) and a target task consisting of vehicle classes plus horse (airplane, automobile, horse, ship, truck). Each task is formulated as 5-way classification with labels remapped to $\{0, 1, 2, 3, 4\}$ to match the model output dimension.

To create a realistic scenario where transfer learning provides meaningful benefit, we use the full training set for the source task ($\approx 25K$ samples, 5K per class) but subsample the target training data to only 5% ($\approx 1.25K$ total samples, roughly 250 per class). This limited-data regime is precisely where transfer learning should provide substantial value, allowing us to cleanly observe the effect of source regularization choices.

We train a small convolutional neural network with two convolutional layers ($3 \rightarrow 32 \rightarrow 64$ channels with 3×3 kernels and 2×2 max-pooling) followed by two fully-connected layers (128 hidden units, dropout 0.25, 5-class output), totaling approximately 530K parameters. For each noise level $\rho \in \{0.0, 0.1, 0.2, 0.3, 0.4\}$ and each source weight decay $\lambda \in \{0, 10^{-5}, 5 \times 10^{-5}, 10^{-4}, 5 \times 10^{-4}, 10^{-3}, 5 \times 10^{-3}, 10^{-2}\}$, we:

- (1) Add label noise to the source training set by randomly flipping labels with probability ρ (while keeping the target task clean)
- (2) Train a source model for 15 epochs using Adam with learning rate 0.001 and L2 weight decay λ
- (3) Evaluate source task performance on the clean source test set
- (4) Initialize a new model from the source weights and fine-tune on the target training data for 8 epochs (fixed weight decay 10^{-4})
- (5) Evaluate target task performance and compare to a from-scratch baseline

We repeat each configuration across 3 random seeds and report average results.

4.1.2. Results. At low noise levels (high SNR), the transfer-optimal source weight decay is consistently larger than the source-optimal choice. For instance, at $\rho = 0.0$, the source-optimal weight decay is 0 (no regularization), while the transfer-optimal choice is 5×10^{-3} . Similarly, at $\rho = 0.1$, source-optimal is 10^{-3} while transfer-optimal is 5×10^{-3} . This pattern matches our theoretical prediction (Corollary 3.9) that high-SNR regimes require stronger regularization for optimal transfer than for source task performance.

As the noise level increases (lower SNR), the gap narrows and eventually reverses. At $\rho = 0.4$, the transfer-optimal weight decay (10^{-3}) is smaller than the source-optimal choice (5×10^{-3}), consistent with the theory’s prediction that low-SNR regimes benefit from weaker regularization for transfer purposes.

Critically, transfer learning provides substantial benefit in this limited-data regime: transfer models achieve 68-75% accuracy on the target task compared to 55-65% for from-scratch baselines, yielding 5-8 percentage point improvements. This meaningful transfer benefit validates that the task design successfully creates a scenario where source regularization choices matter for downstream performance.

4.2. MNIST Experiments.

4.2.1. Experimental Setup. To validate robustness across different architectures and data modalities, we perform a second set of experiments on MNIST. We construct a transfer learning task by splitting the 10 digit classes: source task consists of ‘round’ digits (0, 3, 6, 8, 9), and target task consists of the remaining digits. Each task is formulated as 5-way classification.

We use a simple two-layer multilayer perceptron (MLP) with architecture $784 \rightarrow 128 \rightarrow 64 \rightarrow 5$, totaling approximately 110K parameters. This differs substantially from the convolutional architecture used for CIFAR-10, providing evidence that the phenomenon is not architecture-specific. We use the full MNIST training set for the source task ($\approx 30K$ samples) but subsample the target training data to 10% ($\approx 3K$ samples), again creating a limited-data transfer scenario.

For each noise level $\rho \in \{0.0, 0.1, 0.2, 0.3, 0.4\}$ and each source weight decay $\lambda \in \{0, 10^{-5}, 5 \times 10^{-5}, 10^{-4}, 5 \times 10^{-4}, 10^{-3}, 5 \times 10^{-3}, 10^{-2}\}$, we follow the same protocol as CIFAR-10: add label noise to source task, train source model, evaluate source performance, fine-tune on target task (fixed weight decay 10^{-4}), and compare to from-scratch baseline. We repeat across 10 random seeds.

4.2.2. Results. The MNIST results corroborate the CIFAR-10 findings, demonstrating that the source-optimal versus transfer-optimal misalignment is robust across different datasets and architectures. At the cleanest noise level ($\rho = 0.0$), the source-optimal weight decay is 0 while the transfer-optimal is 5×10^{-3} , again showing that high-SNR regimes benefit from stronger regularization for transfer than for source performance. At the highest noise level ($\rho = 0.4$), the transfer-optimal weight decay (5×10^{-5}) is smaller than the source-optimal choice (5×10^{-4}), confirming the predicted reversal in low-SNR regimes.

Transfer models achieve 96.4-96.5% accuracy on the target task compared to 95.8-96.0% for from-scratch baselines, providing 0.4-0.7 percentage point improvements. While the absolute gains are smaller than CIFAR-10 (due to MNIST’s relative simplicity), the qualitative pattern of SNR-dependent misalignment matches perfectly across both datasets and architectures.

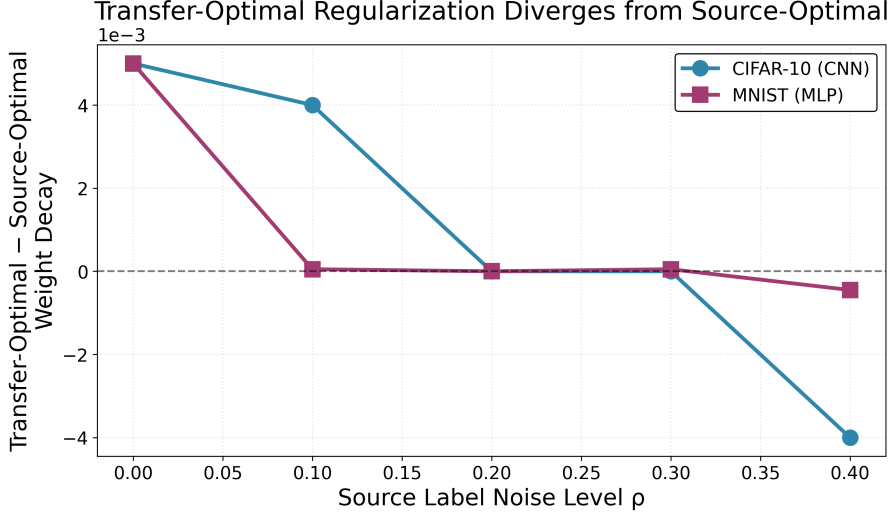


FIGURE 1. Empirical validation on CIFAR-10 and MNIST. The difference between transfer-optimal and source-optimal weight decay (y-axis) is plotted against source label noise level (x-axis). Both datasets exhibit the predicted pattern: positive difference at low noise (high SNR, requiring stronger regularization for transfer) transitioning to negative difference at high noise (low SNR, requiring weaker regularization for transfer).

5. CONCLUSION

We have provided an explicit transfer-versus-scratch boundary for L2-SP ridge that holds at finite p, n and extends to general covariance via deterministic equivalents. In isotropic limits, both ridgeless and ridge, the transfer decision is independent of the target sample size and noise, while the advantage region contracts monotonically as the source noise grows. The boundary reveals that positive transfer depends on the alignment between w_0 and w_1 (in the appropriate geometry) surpassing a threshold dependent on a source bias term and a term that scales with source noise. Optimizing the source model to maximize the positive transfer region yields a unique source ridge τ_0^* that differs generically from the source-task-optimal choice. Counter to standard single-task intuition, transfer learning often requires stronger regularization in high-SNR regimes and weaker regularization in low-SNR regimes with high task alignment.

These results give an analytical foundation for the idea that pretraining optimized for transfer differs fundamentally from pretraining aimed at standalone accuracy. They suggest re-evaluating regularization and objective design in pretraining, foundation-model, and continual-learning pipelines. In particular, practitioners training source models with the goal of downstream transfer should carefully consider the source SNR regime when selecting regularization strength, as the transfer-optimal choice generically differs from what single-task validation would suggest.

Our empirical validation on CIFAR-10 and MNIST provides evidence that this source-optimal versus transfer-optimal misalignment persists beyond the linear regime and is robust across different datasets and architectures. While deep networks trained with SGD exhibit implicit regularization and other effects not captured by our ridge analysis, the

core qualitative pattern matches our predictions consistently: at low noise (high SNR), transfer-optimal weight decay exceeds source-optimal, while at high noise (low SNR), the relationship reverses. The fact that this phenomenon is observable across multiple standard benchmarks with different architectures (convolutional networks for CIFAR-10, MLPs for MNIST) suggests it may have practical relevance for foundation model training pipelines. Practitioners training source models with transfer objectives should consider the source data quality when selecting regularization strength rather than relying solely on source task validation performance.

5.1. Practical Implications. Our results provide several concrete insights for practitioners working with transfer learning systems. First, minimizing source noise is critical for maximizing the region of positive transfer, as the transfer benefit shrinks monotonically with σ_0^2 . This suggests that investing in data cleaning, noise reduction, or improved labeling for the source task can pay significant dividends for downstream transfer, beyond simply improving source task performance. Second, the independence of the transfer decision from target sample size and noise in isotropic settings suggests that if transfer is beneficial for one target dataset size, it remains beneficial across different scales of target data, provided the task structure remains similar. This can simplify model selection in scenarios where target data availability is uncertain or variable.

When tasks exhibit high alignment, the phase transition in optimal regularization strength as a function of SNR provides actionable guidance for model training. In high-SNR regimes where signal dominates noise, one should increase regularization beyond what would be optimal for source task performance alone, effectively trading off some source performance for better transferability. Conversely, in low-SNR regimes where noise is significant, one should reduce regularization relative to the source-optimal value. This counterintuitive guidance reflects the fundamental tension between fitting the source task well and preserving structure that generalizes to related target tasks. Additionally, when task alignment is expected to be positive but weak, our results indicate that the initial model should be trained with higher regularization than is source-optimal, regardless of SNR.

We note here that while our analysis focuses on L2-SP ridge regression, these insights likely extend qualitatively to more complex fine-tuning protocols in deep learning, suggesting that foundation model training pipelines may benefit from regularization strategies that explicitly account for downstream transfer objectives rather than solely optimizing upstream performance.

5.2. Limitations and Scope. Our analysis has several important limitations that should be acknowledged. First, while our theoretical analysis works exclusively with linear models for analytical tractability, our experiments on CIFAR-10 and MNIST suggest the core mechanism persists in nonlinear settings. Nevertheless, the precise functional forms and boundaries we derive are specific to the linear ridge case, and the magnitude of effects in deep networks may differ substantially from our predictions. Second, we assume Gaussian noise and employ either exact isotropy or Bai-Silverstein conditions for our deterministic equivalent results. Real-world data often exhibits non-Gaussian noise, heavy-tailed distributions, and structured covariance that violates these assumptions. Extensions to more general noise models and covariance structures remain important open problems.

Third, we focus on the L2-SP protocol, which penalizes Euclidean distance from the source parameters. This differs from more sophisticated fine-tuning methods that might incorporate task-specific metrics, feature-space regularization, or adaptive penalties based on parameter importance. Additionally, L2-SP represents a closed-form ridge solution, while

practical deep learning relies on iterative optimization via gradient descent. However, the implicit regularization of early-stopped SGD typically keeps parameters close to initialization, qualitatively matching the L2-SP behavior. The recent work of Ghane, Akhtiamov, and Hassibi [9] on gradient-descent-based fine-tuning provides complementary insights for the iterative case, and connecting these perspectives remains an interesting direction.

Finally, our results focus on two-task transfer, whereas many practical scenarios involve continual learning across multiple sequential tasks or multi-task learning with many simultaneous objectives. The interplay between multiple tasks and optimal source regularization represents a rich area for future investigation.

5.3. Future Directions. Several promising directions emerge from this work. First, connecting our ridge-based findings to gradient-descent dynamics in deep learning represents an important bridge to practice. Understanding how implicit regularization in over-parameterized neural networks interacts with the mechanisms we identify could inform training procedures for foundation models. In particular, investigating whether early stopping, learning rate schedules, or architectural choices can implicitly achieve transfer-optimal regularization even when explicit penalties are not used would provide actionable insights for practitioners.

Second, analyzing multi-task and continual learning scenarios where multiple target tasks must be considered simultaneously could reveal how to optimize source training when facing diverse downstream objectives with potentially conflicting requirements. Finally, more extensive empirical validation across diverse architectures, datasets, and transfer scenarios would help assess the robustness of these patterns and guide the development of more sophisticated transfer-optimized training algorithms.

Though derived in the tractable setting of linear ridge regression, our results isolate a fundamental tension between optimizing for source performance versus transfer capability that likely manifests across a broad range of learning systems. By making this tension analytically precise, we hope to inform the design of pretraining objectives that explicitly account for downstream transfer goals.

REFERENCES

- [1] Zhidong Bai and Jack W Silverstein. *Spectral analysis of large dimensional random matrices*, volume 20. Springer, 2010.
- [2] Peter L Bartlett, Philip M Long, Gábor Lugosi, and Alexander Tsigler. Benign overfitting in linear regression. *Proceedings of the National Academy of Sciences*, 117(48):30063–30070, 2020.
- [3] Mikhail Belkin, Daniel Hsu, Siyuan Ma, and Soumik Mandal. Reconciling modern machine-learning practice and the classical bias–variance trade-off. *Proceedings of the National Academy of Sciences*, 116(32):15849–15854, 2019.
- [4] Romain Couillet and Merouane Debbah. *Random matrix methods for wireless communications*. Cambridge University Press, 2011.
- [5] Yehuda Dar and Richard G Baraniuk. Double double descent: On generalization errors in transfer learning between linear regression tasks. *SIAM Journal on Mathematics of Data Science*, 4(4):1447–1472, 2022.
- [6] Yehuda Dar, Daniel LeJeune, and Richard G Baraniuk. The common intuition to transfer learning can win or lose: Case studies for linear regression. *SIAM Journal on Mathematics of Data Science*, 6(2):454–480, 2024.
- [7] Oussama Difallah and Yue M Lu. Phase transitions in transfer learning for high-dimensional perceptrons. *Entropy*, 23(4):400, 2021.
- [8] Edgar Dobriban and Stefan Wager. High-dimensional asymptotics of prediction: Ridge regression and classification. *The Annals of Statistics*, 46(1):247–279, 2018.
- [9] Reza Ghane, Danil Akhtiamov, and Babak Hassibi. Universality in transfer learning for linear models. *Advances in Neural Information Processing Systems*, 37:125729–125779, 2024.

- [10] Trevor Hastie, Andrea Montanari, Saharon Rosset, and Ryan J Tibshirani. Surprises in high-dimensional ridgeless least squares interpolation. *Annals of statistics*, 50(2):949, 2022.
- [11] James Kirkpatrick, Razvan Pascanu, Neil Rabinowitz, Joel Veness, Guillaume Desjardins, Andrei A Rusu, Kieran Milan, John Quan, Tiago Ramalho, Agnieszka Grabska-Barwinska, et al. Overcoming catastrophic forgetting in neural networks. *Proceedings of the national academy of sciences*, 114(13):3521–3526, 2017.
- [12] Alex Krizhevsky, Geoffrey Hinton, et al. Learning multiple layers of features from tiny images. Technical report, University of Toronto, 2009.
- [13] Andrew K Lampinen and Surya Ganguli. An analytic theory of generalization dynamics and transfer learning in deep linear networks. *arXiv preprint arXiv:1809.10374*, 2018.
- [14] Javan Tahir, Surya Ganguli, and Grant M Rotskoff. Features are fate: a theory of transfer learning in high-dimensional regression. *arXiv preprint arXiv:2410.08194*, 2024.
- [15] LI Xuhong, Yves Grandvalet, and Franck Davoine. Explicit inductive bias for transfer learning with convolutional networks. In *International conference on machine learning*, pages 2825–2834. PMLR, 2018.
- [16] Fan Yang, Hongyang R Zhang, Sen Wu, Christopher Re, and Weijie J Su. Precise high-dimensional asymptotics for quantifying heterogeneous transfers. *Journal of Machine Learning Research*, 26(113):1–88, 2025.

6. APPENDIX

Here we will re-state and prove the relevant Lemmas and Theorems mentioned above.

6.1. Finite Sample Risk Formulas. We begin by re-writing our L2-SP transfer learning estimator for the reader's convenience:

$$\hat{\beta}_1^{\text{TL}}(\lambda_1 \mid \hat{\beta}_0) = (X_1^\top X_1 + \lambda_1 I)^{-1} \left(X_1^\top y_1 + \lambda_1 \hat{\beta}_0(\lambda_0) \right).$$

We additionally note that expected risk can be computed by:

$$R(\beta) = E \left[\|\beta - w_1\|_{\Sigma_1}^2 \right].$$

We can now prove the first important Lemma:

Lemma 3.2 The expected risk of the transfer estimator decomposes into pure bias, variance induced by the β_0 prior, and variance induced by estimation error:

$$R^{\text{TL}}(\lambda_1) = B^{\text{TL}}(\lambda_1) + \sigma_0^2 V_0^{\text{TL}}(\lambda_1) + \sigma_1^2 V_1^{\text{TL}}(\lambda_1)$$

with:

$$\begin{aligned} B^{\text{TL}}(\lambda_1) &= \lambda_1^2 \mathbb{E} \left[\|M_{\lambda_1}^{(1)} M_{\lambda_0}^{(0)} X_0^\top X_0 w_0 - M_{\lambda_1}^{(1)} w_1\|_{\Sigma_1}^2 \right] \\ V_0^{\text{TL}}(\lambda_1) &= \lambda_1^2 \mathbb{E} \left[\|M_{\lambda_1}^{(1)} M_{\lambda_0}^{(0)} X_0^\top\|_{\Sigma_1, F}^2 \right] \\ V_1^{\text{TL}}(\lambda_1) &= \mathbb{E} \left[\|M_{\lambda_1}^{(1)} X_1^\top\|_{\Sigma_1, F}^2 \right]. \end{aligned}$$

Proof. We verify the decomposition as follows. First note:

$$\begin{aligned} \hat{\beta}_1^{\text{TL}}(\lambda \mid \hat{\beta}_0) - w_1 &= \lambda M_\lambda^{(1)} \hat{\beta}_0^S(\lambda_0) + \hat{\beta}_1^S(\lambda) - w_1 \\ &= \lambda M_\lambda^{(1)} M_{\lambda_0}^{(0)} X_0^\top y_0 + M_\lambda^{(1)} X_1^\top y_1 - w_1 \\ &= \lambda M_\lambda^{(1)} M_{\lambda_0}^{(0)} X_0^\top X_0 w_0 + \lambda M_\lambda^{(1)} M_{\lambda_0}^{(0)} X_0^\top \epsilon_0 + M_\lambda^{(1)} X_1^\top X_1 w_1 + M_\lambda^{(1)} X_1^\top \epsilon_1 - w_1 \\ &= \left(\lambda M_\lambda^{(1)} M_{\lambda_0}^{(0)} X_0^\top X_0 + (M_\lambda^{(1)} X_1^\top X_1 - I) \right) w_1 + \left(\lambda M_\lambda^{(1)} M_{\lambda_0}^{(0)} X_0^\top \right) \epsilon_0 + \left(M_\lambda^{(1)} X_1^\top \right) \epsilon_1. \end{aligned}$$

We then take expectation of the squared Σ_1 norm of the above expression and since ϵ_0, ϵ_1 are taken independently with mean 0, the cross terms cancel and we are left with the desired result. \square

We now remind the reader that the expected risk of the standard Ridge estimator is

$$R^S(\lambda_1) = \lambda_1^2 \mathbb{E} \left[\|M_{\lambda_1}^{(1)} w_1\|_{\Sigma_1}^2 \right] + \sigma_1^2 \mathbb{E} \left[\|M_{\lambda_1}^{(1)} X_1^\top\|_{\Sigma_1, F}^2 \right].$$

We can therefore compare these quantities to identify when we expect Transfer to outperform training from scratch.

Theorem 3.3. In the finite sample case with $\lambda_1 > 0$, we gain benefit from transfer learning ($R^{\text{TL}}(\lambda_1) < R^S(\lambda_1)$) if and only if:

$$2\mathbb{E} \left[\langle M_{\lambda_1}^{(1)} M_{\lambda_0}^{(0)} X_0^\top X_0 w_0, M_{\lambda_1}^{(1)} w_1 \rangle_{\Sigma_1} \right] > \mathbb{E} \left[\|M_{\lambda_1}^{(1)} M_{\lambda_0}^{(0)} X_0^\top X_0 w_0\|_{\Sigma_1}^2 \right] + \sigma_0^2 \mathbb{E} \left[\|M_{\lambda_1}^{(1)} M_{\lambda_0}^{(0)} X_0^\top\|_{\Sigma_1, F}^2 \right].$$

Proof. First we notice the σ_1 terms of $R^S(\lambda_1)$ and $R^{\text{TL}}(\lambda_1 \mid \beta_0)$ exactly cancel. We are therefore left with

$$\begin{aligned} R^S(\lambda) - R^{\text{TL}}(\lambda) &= \mathbb{E} \left[\|(M_\lambda^{(1)} X_1^\top X_1 - I) w_1\|_{\Sigma_1}^2 \right] - \mathbb{E} \left[\|\lambda M_\lambda^{(1)} M_{\lambda_0}^{(0)} X_0^\top X_0 w_0 + (M_\lambda^{(1)} X_1^\top X_1 - I) w_1\|_{\Sigma_1}^2 \right] \\ &\quad - \sigma_0^2 \lambda^2 \mathbb{E} \left[\|M_\lambda^{(1)} M_{\lambda_0}^{(0)} X_0^\top\|_{\Sigma_1, F}^2 \right] \end{aligned}$$

$$\begin{aligned}
&= -\mathbb{E} \left[\|\lambda M_{\lambda}^{(1)} M_{\lambda_0}^{(0)} X_0^\top X_0 w_0\|_{\Sigma_1}^2 \right] - 2\lambda \mathbb{E} \left[\langle (M_{\lambda}^{(1)} X_1^\top X_1 - I) w_1, M_{\lambda}^{(1)} M_{\lambda_0}^{(0)} X_0^\top X_0 w_0 \rangle_{\Sigma_1} \right] \\
&\quad - \sigma_0^2 \lambda^2 \mathbb{E} \left[\|M_{\lambda}^{(1)} M_{\lambda_0}^{(0)} X_0^\top\|_{\Sigma_1, F}^2 \right].
\end{aligned}$$

We note here that $(M_{\lambda}^{(1)} X_1^\top X_1 - I) = -\lambda M_{\lambda}^{(1)}$ and thus we have

$$\mathbb{E} \left[\langle (M_{\lambda}^{(1)} X_1^\top X_1 - I) w_1, M_{\lambda}^{(1)} M_{\lambda_0}^{(0)} X_0^\top X_0 w_0 \rangle_{\Sigma_1} \right] = -\lambda \mathbb{E} \left[\langle M_{\lambda}^{(1)} w_1, M_{\lambda}^{(1)} M_{\lambda_0}^{(0)} X_0^\top X_0 w_0 \rangle_{\Sigma_1} \right].$$

After some algebra and canceling the common λ^2 terms, we arrive at our desired inequality. \square

Corollary 3.4 In the finite case, if $\Sigma_i = I$ and $\lambda_1 = \lambda_0 = 0$, and X_i is taken to be Gaussian, then $R^{TL}(0) < R^S(0)$ if and only if:

$$2 \langle w_0, w_1 \rangle > \|w_0\|^2 + \sigma_0^2 \frac{p}{p - n_0 - 1}.$$

Proof. We first note

$$\lim_{\lambda \searrow 0} M_{\lambda_1}^{(1)} = \lim_{\lambda \searrow 0} (X_1^\top X_1 + \lambda I)^{-1} = (X_1^\top X_1)^+ = I - X_1^+ X_1.$$

By conditioning on X_0 and taking expectation with respect to X_1 , the projection $I - X_1^+ X_1$ introduces a common factor of $\frac{p - n_1}{p}$ to all terms involving w_1 or the X_0 -dependent prior (due to the isotropy of X_1). Specifically, for any fixed vector v , $\mathbb{E}_{X_1} [\|(I - X_1^+ X_1)v\|^2] = \frac{p - n_1}{p} \|v\|^2$. We can thus eliminate the target projection effects from the expression. We are then left with:

$$2\mathbb{E} \left[\langle M_{\lambda_0}^{(0)} X_0^\top X_0 w_0, w_1 \rangle \right] > \mathbb{E} \left[\|M_{\lambda_0}^{(0)} X_0^\top X_0 w_0\|_{\Sigma_1}^2 \right] + \sigma_0^2 \mathbb{E} \left[\|M_{\lambda_0}^{(0)} X_0^\top\|_{\Sigma_1, F}^2 \right].$$

We now note that

$$\lim_{\lambda_0 \searrow 0} M_{\lambda_0}^{(0)} X_0^\top = X_0^+,$$

and thus we have

$$2\mathbb{E} [\langle X_0^+ X_0 w_0, w_1 \rangle] > \mathbb{E} [\|X_0^+ X_0 w_0\|_{\Sigma_1}^2] + \sigma_0^2 \mathbb{E} [\|X_0^+\|_{\Sigma_1, F}^2].$$

We note here that since $\Sigma_0 = I$ we have $E [X_0^+ X_0] = \frac{n_0}{p} I$. Additionally, $E [\|X_0^+\|_F^2] = \frac{n_0}{p - n_0 - 1}$. We can now take expectation to see

$$2 \frac{n_0}{p} \langle w_0, w_1 \rangle > \frac{n_0}{p} \|w_0\|^2 + \sigma_0^2 \frac{n_0}{p - n_0 - 1}.$$

By multiplying by $\frac{p}{n_0}$ we arrive at the desired result. \square

6.2. Deterministic Equivalents and Asymptotics. We will now examine asymptotics for the ridge phase transition identified above and use deterministic equivalents to understand the limiting phase transition. To establish the core deterministic equivalents, we must first let $\tau_i = \lambda_i/n_i$, and we define the following ridge resolvent:

$$Q_i(\tau_i) = (\tau_i I + \delta_i(\tau_i) \Sigma_i)^{-1}$$

where $\delta_i(\tau_i)$ is the unique positive solution to the Silverstein fixed-point equation

$$\delta_i(\tau_i) = n_i \text{Tr} \left(\Sigma_i (\tau_i I + \gamma_i \delta_i(\tau_i) \Sigma_i)^{-1} \right), \text{ where } \gamma_i = \lim p/n_i.$$

Observation 3.5 Under standard Bai-Silverstein conditions ([1]), as $p, n_i \rightarrow \infty$ with $p/n_i \rightarrow \gamma_i$:

$$\begin{aligned} \lambda_1 M_{\lambda_1}^{(1)} &\asymp \tau_1 Q_1(\tau_1), \\ M_{\lambda_0}^{(0)} X_0^\top &\asymp n_0^{-1} \frac{1}{\tau_0(1 + \delta_0(\tau_0))} X_0^\top, \text{ and} \\ M_{\lambda_0}^{(0)} X_0^\top X_0 M_{\lambda_0}^{(0)} &\asymp n_0^{-1} (Q_0(\tau_0) - \tau_0 Q_0(\tau_0)^2). \end{aligned}$$

Proof. These equivalences follow from standard results in [1]. Specifically, under the Bai-Silverstein conditions, the empirical resolvent $(X_i^\top X_i/n_i + \lambda_i I)^{-1}$ admits the deterministic equivalent $n_i^{-1} Q_i(\tau_i) = n_i^{-1} (\tau_i I + \delta_i(\tau_i) \Sigma_i)^{-1}$, where $\delta_i(\tau_i)$ is the unique positive solution to the Silverstein fixed-point equation. By dividing by λ_1 we arrive at the first deterministic equivalence.

On the sample side we know

$$M_{\lambda_0}^{(0)} X_0^\top = X_0^\top M_{\lambda_0}^{(0)} = n_0^{-1} X_0^\top (X_0^\top X_0/n_0 + \lambda_0 I)^{-1},$$

and the second deterministic equivalent follows.

Finally we use the following fact:

$$M_{\lambda_0}^{(0)} X_0^\top X_0 M_{\lambda_0}^{(0)} = M_{\lambda_0}^{(0)} ((X_0^\top X_0 + \lambda_0 I) - \lambda_0 I) M_{\lambda_0}^{(0)} = M_{\lambda_0}^{(0)} - \lambda_0 (M_{\lambda_0}^{(0)})^2.$$

From this it is easy to see the third deterministic equation holds. \square

Finally, define

$$t(\tau_0, \tau_1) = \lim_{p \rightarrow \infty} p^{-1} \text{Tr} (Q_1(\tau_1) \Sigma_1 Q_1(\tau_1) (Q_0(\tau_0) - \tau_0 Q_0(\tau_0)^2)),$$

which we know exists under the Bai-Silverstein assumptions. By independence of X_0 and X_1 , we may substitute these in to the results from Theorem 3.3 to arrive at the following asymptotic decision criterion:

Theorem 3.6 In the asymptotic limit, we gain benefit from transfer learning ($R^{TL}(\lambda_1) < R^S(\lambda_1)$) if and only if:

$$2 \langle Q_1(\tau_1)(I - \tau_0 Q_0(\tau_0))w_0, Q_1(\tau_1)w_1 \rangle_{\Sigma_1} > \|Q_1(\tau_1)(I - \tau_0 Q_0(\tau_0))w_0\|_{\Sigma_1}^2 + \sigma_0^2 \gamma_0 t(\tau_0, \tau_1).$$

Proof. This result follows directly from substituting the deterministic equivalents from Observation 3.5 into the results from Theorem 3.3 combined with the independence of X_1 and X_0 . \square

Corollary 3.7 In the isotropic case where $\Sigma_0 = \Sigma_1 = I$, we (asymptotically) gain benefit from transfer learning ($R^{TL}(\lambda_1) < R^S(\lambda_1)$) if and only if:

$$2 \langle w_0, w_1 \rangle > \gamma_0 a_0^2 \|w_0\|^2 + \sigma_0^2 \gamma_0 a_0,$$

where

$$a_0 = \frac{-\tau_0 + \sqrt{\tau_0^2 + 4\gamma_0}}{2\gamma_0}.$$

Proof. We note that when $\Sigma_i = I$, we know by [1] that $Q_i(\tau_i) = a_i I$ where

$$a_i = \frac{-\tau_i + \sqrt{\tau_i^2 + 4\gamma_i}}{2\gamma_i}.$$

We can substitute this in to the relevant quantities from Theorem 3.6 to see:

$$2 \langle Q_1(\tau_1)(I - \tau_0 Q_0(\tau_0))w_0, Q_1(\tau_1)w_1 \rangle_{\Sigma_1} = 2 \langle a_1(I - a_0 I)w_0, a_1 w_1 \rangle \text{ and}$$

$$\|Q_1(\tau_1)(I - \tau_0 Q_0(\tau_0))w_0\|_{\Sigma_1}^2 = \|a_1(I - a_0 I)w_0\|^2.$$

We now examine

$$\begin{aligned} t(\tau_0, \tau_1) &= \lim_{p \rightarrow \infty} p^{-1} \text{Tr} (a_1^2 I (a_0 I - \tau_0 a_0^2 I)) \\ &= a_1^2 \text{Tr} (a_0 I - \tau_0 a_0^2 I) / p \\ &= a_1^2 (a_0 - \tau_0 a_0^2) \end{aligned}$$

By the identity $a_0 - \tau_0 a_0^2 = a_0(1 - \tau_0 a_0)$ and from the fact that $(1 - \tau_0 a_0) = \gamma_0 a_0^2$ (since $a_0(\tau_0 + \gamma_0 a_0) = 1$), we find

$$t(\tau_0, \tau_1) = a_1^2 a_0 (1 - \tau_0 a_0) = a_1^2 \gamma_0 a_0^3.$$

We now substitute these results into the second inequality in Theorem 3.6 and after canceling the common a_1^2 terms we conclude our proof. \square

Theorem 3.8 In the asymptotic setting with isotropic data and fixed source model overparameterization γ_0 , for any fixed target task alignment $\rho = \langle w_0, w_1 \rangle$, there exists a unique source ridge penalty τ_0^* that maximizes the transfer benefit $\Delta R = R^S - R^{TL}$. Additionally, outside of a measure-zero set of parameters, the optimal τ_0^* for transfer learning differs from the optimal ridge penalty for Task 0 performance.

Proof. We seek to maximize the asymptotic risk benefit $\Delta R(\tau_0) = R^S - R^{TL}(\tau_0)$. Since R^S is independent of τ_0 , this is equivalent to minimizing $R^{TL}(\tau_0)$. Using the isotropic deterministic equivalents, the transfer risk asymptotically converges to:

$$R^{TL}(\tau_0) \asymp \|w_1\|^2 - 2\gamma_0 a_0(\tau_0)^2 \langle w_0, w_1 \rangle + \gamma_0^2 a_0(\tau_0)^4 \|w_0\|^2 + \sigma_0^2 \gamma_0^2 a_0(\tau_0)^3,$$

where $a_0(\tau_0) = (-\tau_0 + \sqrt{\tau_0^2 + 4\gamma_0})/(2\gamma_0)$ maps $\tau_0 \in [0, \infty)$ bijectively to $a_0 \in (0, 1/\sqrt{\gamma_0}]$.

Optimizing with respect to τ_0 is equivalent to optimizing with respect to a_0 . Let

$$f(a_0) = -2\gamma_0 \langle w_0, w_1 \rangle a_0^2 + \gamma_0^2 \|w_0\|^2 a_0^4 + \sigma_0^2 \gamma_0^2 a_0^3.$$

We seek to minimize $f(a_0)$ over the feasible interval. Taking the derivative with respect to a_0 :

$$f'(a_0) = -4\gamma_0 \langle w_0, w_1 \rangle a_0 + 4\gamma_0^2 \|w_0\|^2 a_0^3 + 3\sigma_0^2 \gamma_0^2 a_0^2 = a_0 \gamma_0 (-4 \langle w_0, w_1 \rangle + 4\gamma_0 \|w_0\|^2 a_0^2 + 3\sigma_0^2 \gamma_0 a_0).$$

Setting $f'(a_0) = 0$ yields a quadratic equation in a_0 (ignoring the trivial $a_0 = 0$ root corresponding to infinite regularization). We let a_0^* be the unique solution to $f'(a_0) = 0$ in the interval $(0, 1/\sqrt{\gamma_0}]$ and note that it must be:

$$a_0^* = \frac{-3\sigma_0^2 \gamma_0 + \sqrt{9\sigma_0^4 \gamma_0^2 + 64\gamma_0 \|w_0\|^2 \langle w_0, w_1 \rangle}}{8\gamma_0 \|w_0\|^2}.$$

Denote τ_0^* as the corresponding regularization parameter to this a_0^* and we note that since the a_0^2 and a_0 terms of f are positive, τ_0^* must be the unique regularization penalty that minimizes downstream risk.

To show this τ_0^* generically differs from source-optimal regularization, we define the source optimal a_0 :

$$a_0^S = a_0 \left(\frac{\gamma_0 \sigma_0^2}{\|w_0\|^2} \right) = \frac{-\tau_0 + \sqrt{\tau_0^2 + 4\gamma_0}}{2\gamma_0}.$$

After some algebra, we can see that $a_0^* = a_0^S$ if and only if

$$\sigma_0^2 \gamma_0 + \sqrt{9\sigma_0^4 \gamma_0^2 + 64\gamma_0 \|w_0\|^2 \langle w_0, w_1 \rangle} = \sqrt{16\sigma_0^4 \gamma_0^2 + 64\gamma_0 \|w_0\|^4}.$$

Since this equation holds for a Lebesgue measure zero set on the parameter space $(\gamma_0, \sigma_0^2, \|w_0\|^2, \rho = \langle w_0, w_1 \rangle)$, we can conclude the desired result. \square

Corollary 3.9 Assume $\|w_0\|^2 > \langle w_0, w_1 \rangle > 0$.

If $\langle w_0, w_1 \rangle < \frac{3}{4}\|w_0\|^2$, then $\tau_0^* > \frac{\gamma_0\sigma_0^2}{\|w_0\|^2}$ (transfer optimal always requires stronger regularization when the tasks have poor alignment).

However, with sufficient alignment ($\langle w_0, w_1 \rangle > \frac{3}{4}\|w_0\|^2$) there exists an noise threshold $\sigma_0^* > 0$ identified by

$$(\sigma_0^*)^2 = \frac{2(\|w_0\|^4 - \|w_0\|^2 \langle w_0, w_1 \rangle)}{\sqrt{\gamma_0(\|w_0\|^2 \langle w_0, w_1 \rangle - \frac{3}{4}\|w_0\|^4)}}$$

such that:

- If $\sigma_0 < \sigma_0^*$, then $\tau_0^* > \frac{\gamma_0\sigma_0^2}{\|w_0\|^2}$ (stronger regularization than source-optimal).
- If $\sigma_0 > \sigma_0^*$, then $\tau_0^* < \frac{\gamma_0\sigma_0^2}{\|w_0\|^2}$ (weaker regularization than source-optimal).

Proof. Let a_0^S be defined as in the proof of Theorem 3.8. We now define the following function:

$$f(\sigma_0) = \sigma_0^2\gamma_0 + \sqrt{9\sigma_0^4\gamma_0^2 + 64\gamma_0\|w_0\|^2 \langle w_0, w_1 \rangle} - \sqrt{16\sigma_0^4\gamma_0^2 + 64\gamma_0\|w_0\|^4}.$$

Note here that if $f(\sigma_0) > 0$, then $a_0^* > a_0^S$ (and thus $\tau_0^* < \frac{\gamma_0\sigma_0^2}{\|w_0\|^2}$; the case is similar with $f(\sigma_0) < 0$). We now note that $f(0) < 0$ since $\langle w_0, w_1 \rangle < \|w_0\|^2$, and thus regardless of task alignment, in the noiseless case we know $\tau_0^* > \frac{\gamma_0\sigma_0^2}{\|w_0\|^2}$.

We now examine when $f(\sigma_0) = 0$. For ease of notation let $x = \sigma_0^2\gamma_0$, $C = 64\gamma_0\|w_0\|^2 \langle w_0, w_1 \rangle$, and $D = 64\gamma_0\|w_0\|^4$. The equation $f(\sigma_0) = 0$ becomes:

$$x + \sqrt{9x^2 + C} = \sqrt{16x^2 + D}.$$

Squaring both sides, isolating the radical term, and squaring again yields:

$$\begin{aligned} x^2 + (9x^2 + C) + 2x\sqrt{9x^2 + C} &= 16x^2 + D \\ 2x\sqrt{9x^2 + C} &= 6x^2 + (D - C) \\ 4x^2(9x^2 + C) &= (6x^2 + (D - C))^2 \\ 36x^4 + 4Cx^2 &= 36x^4 + 12(D - C)x^2 + (D - C)^2. \end{aligned}$$

Canceling the $36x^4$ terms leaves a linear equation in x^2 :

$$4Cx^2 = 12(D - C)x^2 + (D - C)^2 \implies x^2(16C - 12D) = (D - C)^2.$$

Solving for x , we find a unique positive solution exists if and only if $16C > 12D$, or equivalently $4C > 3D$. Substituting back the definitions of C and D :

$$4(64\gamma_0\|w_0\|^2 \langle w_0, w_1 \rangle) > 3(64\gamma_0\|w_0\|^4) \implies \langle w_0, w_1 \rangle > \frac{3}{4}\|w_0\|^2.$$

Thus, a valid crossover point σ_0^* exists if and only if the task alignment exceeds this threshold and an explicit representation for σ_0^* can be found from this expression:

$$(\sigma_0^*)^2 = \frac{2(\|w_0\|^4 - \|w_0\|^2 \langle w_0, w_1 \rangle)}{\sqrt{\gamma_0(\|w_0\|^2 \langle w_0, w_1 \rangle - \frac{3}{4}\|w_0\|^4)}}$$

\square